Supporting Information

Oil-free Acoustofluidic Droplet Generation for Multicellular Tumor Spheroid Culture

Jacqueline A. De Lora[1#], Frank A. Fencl[1#], Aidira D.Y. Macias Gonzalez[1#], Alireza Bandegi[2], Reza Foudazi[2], Gabriel P. Lopez[1], Andrew P. Shreve[1,*], Nick J. Carroll[1,*]

[1]Department of Chemical and Biological Engineering and Center for Biomedical Engineering, University of New Mexico, Albuquerque, NM, USA

[2]Department of Chemical and Materials Engineering, New Mexico State University, Las Cruces, NM, USA

[#]Equal Contributors

Corresponding Authors

* E-mail: shreve@unm.edu (A.P.S.)

* E-mail: ncarroll@unm.edu (N.J.C.)

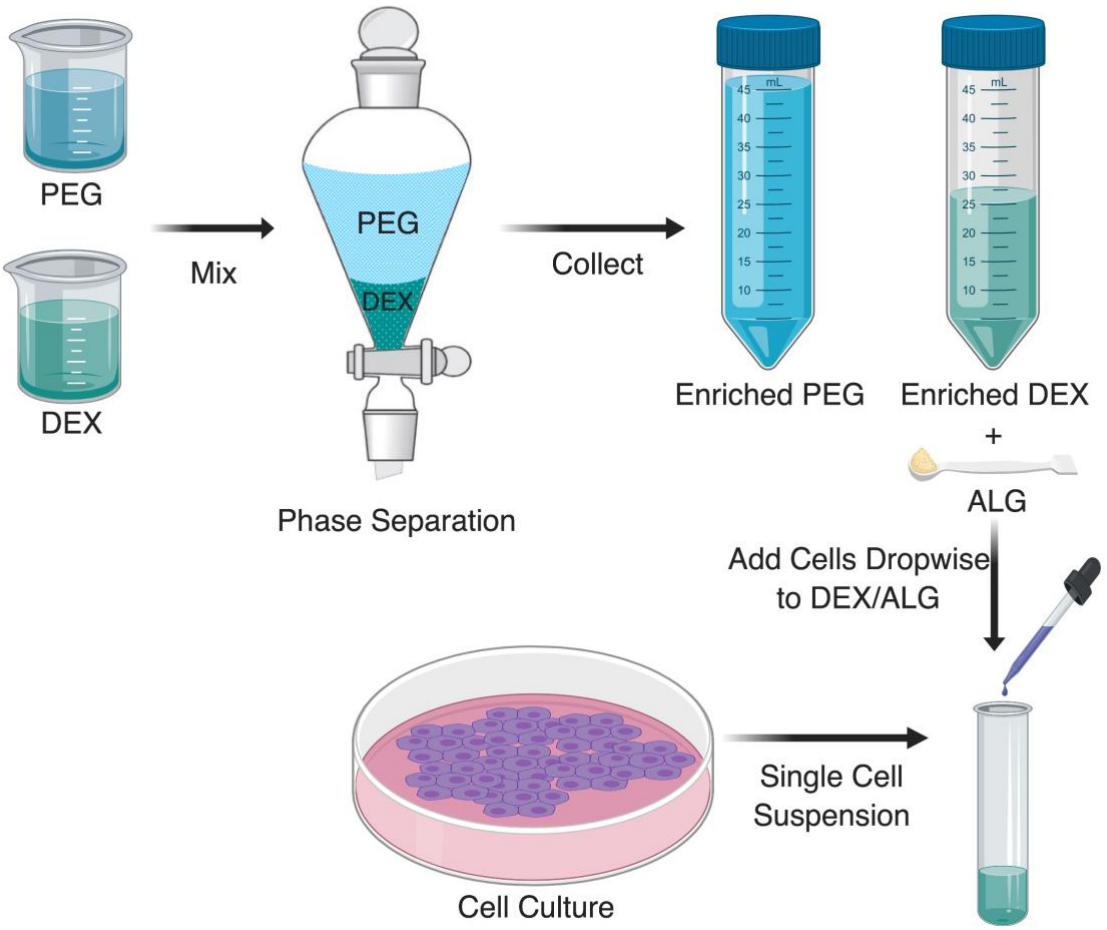

Figure S1. ATPS process illustration depicting the thermodynamic phase separation of the PEG and DEX solutions in a separatory funnel, mixing in 0.5% ALG to form a gelling inner fluid, and the dropwise addition of cells to the DEX/ALG to form a single cell suspension.

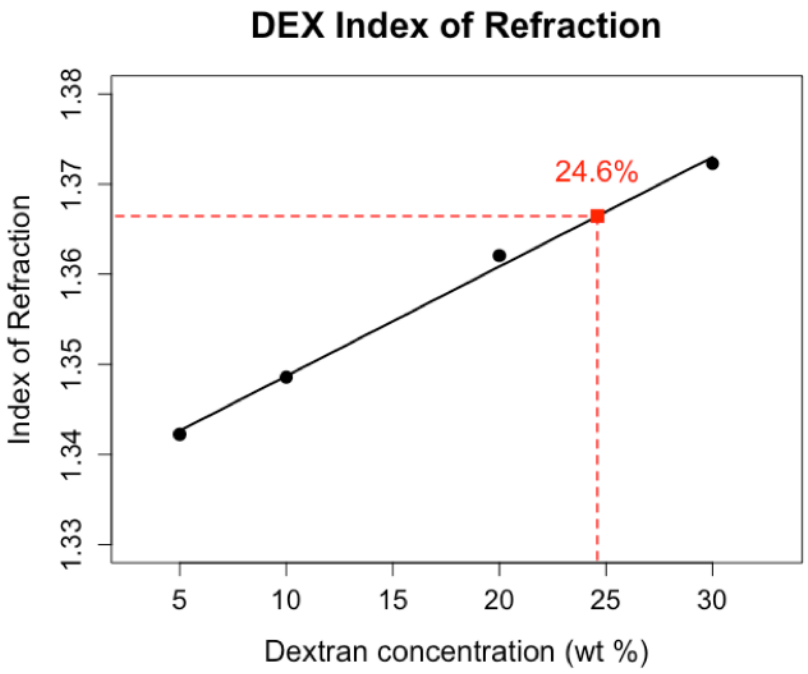

Figure S2. Calibration data generated by measuring the refractive index of 5%, 10%, 20% and 30% w/w dextran in HEPES buffer demonstrates a linear relationship between the concentration of dextran and the index of refraction (black data points and line). The concentration of dextran in the DEX phase (red square and dashed lines) is determined using the calibration curve (black circles and line), resulting in a value of ≈24.6%.

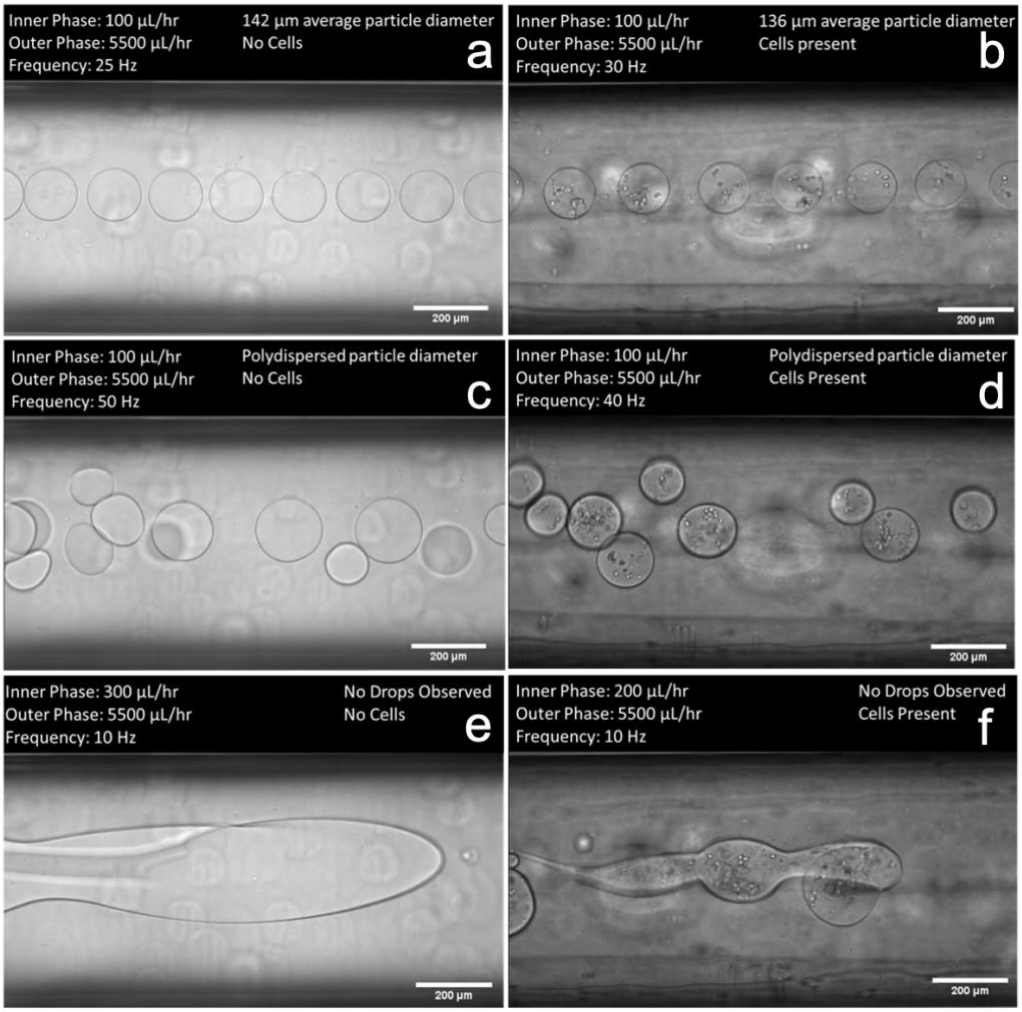

Figure S3. Representative brightfield microscopy images of monodisperse (a and b), polydisperse (c and d), or lack of droplet formation (e and f) taken 5 cm downstream of the nozzles in the acoustofluidic device. The images on the left-hand side do not have cells present in the DEX/ALG whereas the images on the right-hand side have cells present.

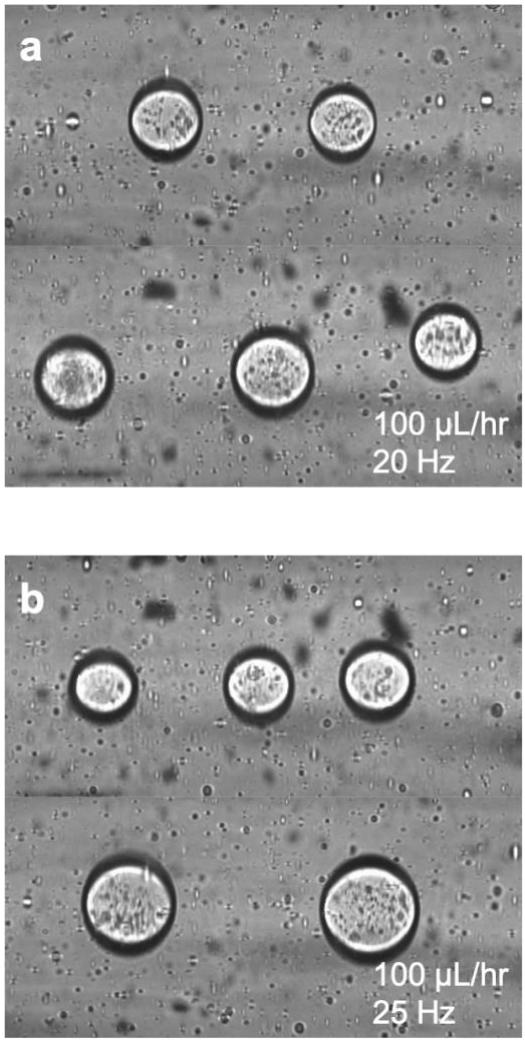

Figure S4. Representative brightfield microscopy images of droplets formed by actuation of the speaker using smartphone control, taken downstream of the nozzles in the acoustofluidic device. The model flow and frequency acoustic actuation parameters (a and b) are chosen given the results of our analysis using an extension of Plateau-Rayleigh theory.

a

Compensation Matrix		
	BL1	**BL2**
BL1	100.00	8.10
BL2	19.46	100.00
BL1	-101.60	8.23
BL2	19.78	-101.60

b

	DEAD	**LIVE**	**DEX/ALG**
%LIVE	6%	87%	75%
%DEAD	93%	10%	23%

Figure S5. Flow cytometry compensation matrix (a) and viability percentages (b). The compensation matrix is used to filter overlapping fluorescent signal in our two-color assay. The percentage of live and dead from the controls and experimental group is measured by gating.

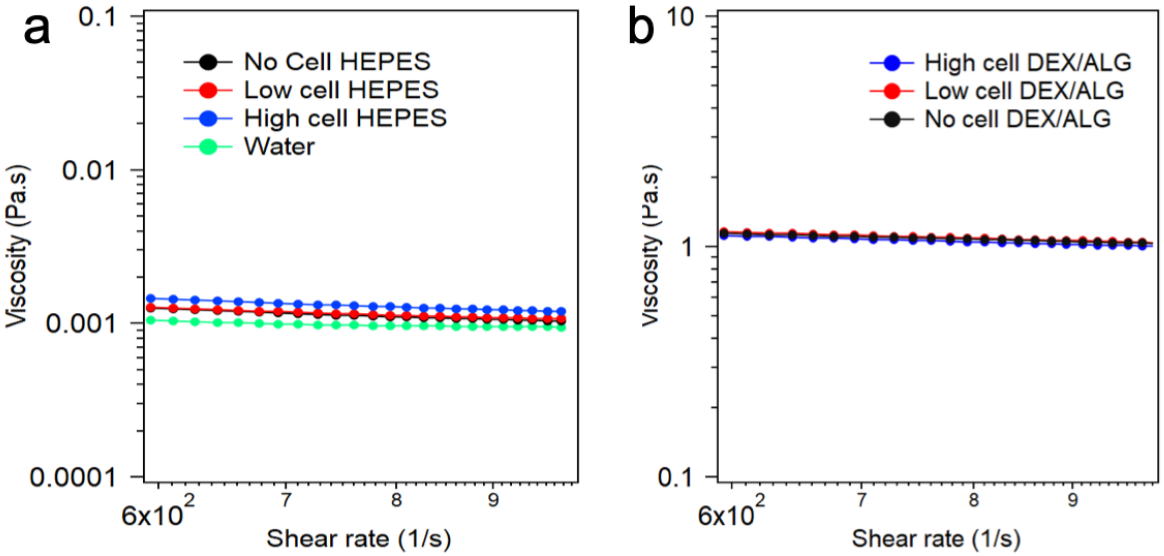

c

Solution	Dynamic Viscosity (Pa. s)	Relative Viscosity (with cell/without cell)
DEX/Alginate No cell	1.25 ± 0.5	1.00
DEX/Alginate Low cell	1.3 ± 0.5	1.02
DEX/Alginate High cell	1.35 ± 0.5	1.04
HEPES No cell	0.0012 ± 0.002	1.00
HEPES Low cell	0.0012 ± 0.002	1.00
HEPES High cell	0.0013 ± 0.002	1.08

Figure S6. The rheology results from flow ramp experiments to measure the effect of cell concentration on solution viscosity (a and b). The control group (a) demonstrates that the solution viscosity is not influenced by the presence of cells in HEPES buffer. Similarly, cell concentration does not influence the DEX/ALG solution, but the overall viscosity of the solution is ~three orders of magnitude higher (b). Table summarizing the dynamic and relative viscosities for the DEX/ALG with no, low, and high cell concentrations in comparison to the control HEPES buffer with no, low and high cell concentrations (c).

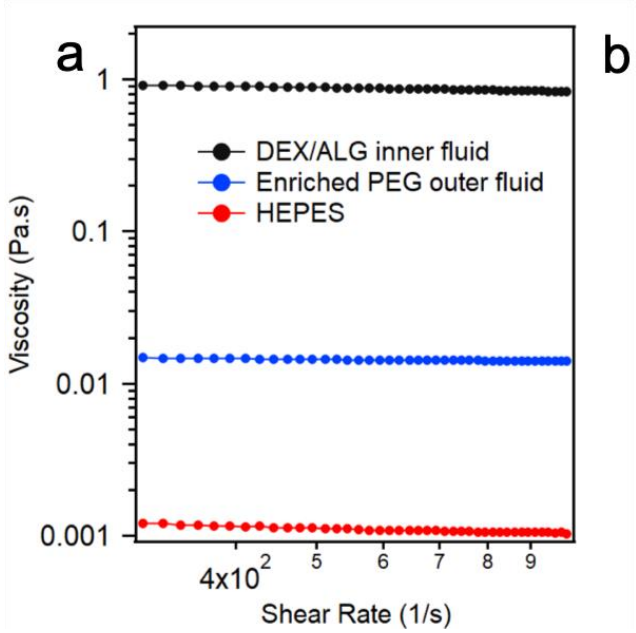

b

Sample	Viscosity (Pa.s)
DEX/ALG inner Fluid	0.9
Enriched PEG	0.012
25 mM HEPES	0.0011

Figure S7. The rheology results from the flow ramp experiment using all components of our ATPS. This result validates the increased viscosity observed when comparing the control solution and the DEX/ALG, HEPES buffer (bottom curve, red) and DEX/ALG inner fluid (top curve, black). The PEG outer fluid (middle curve, blue) is also measured to provide a viscosity measurement for enriched PEG (a). These measured viscosity values (b) are used in our analysis based on an extension of Plateau Rayleigh theory.

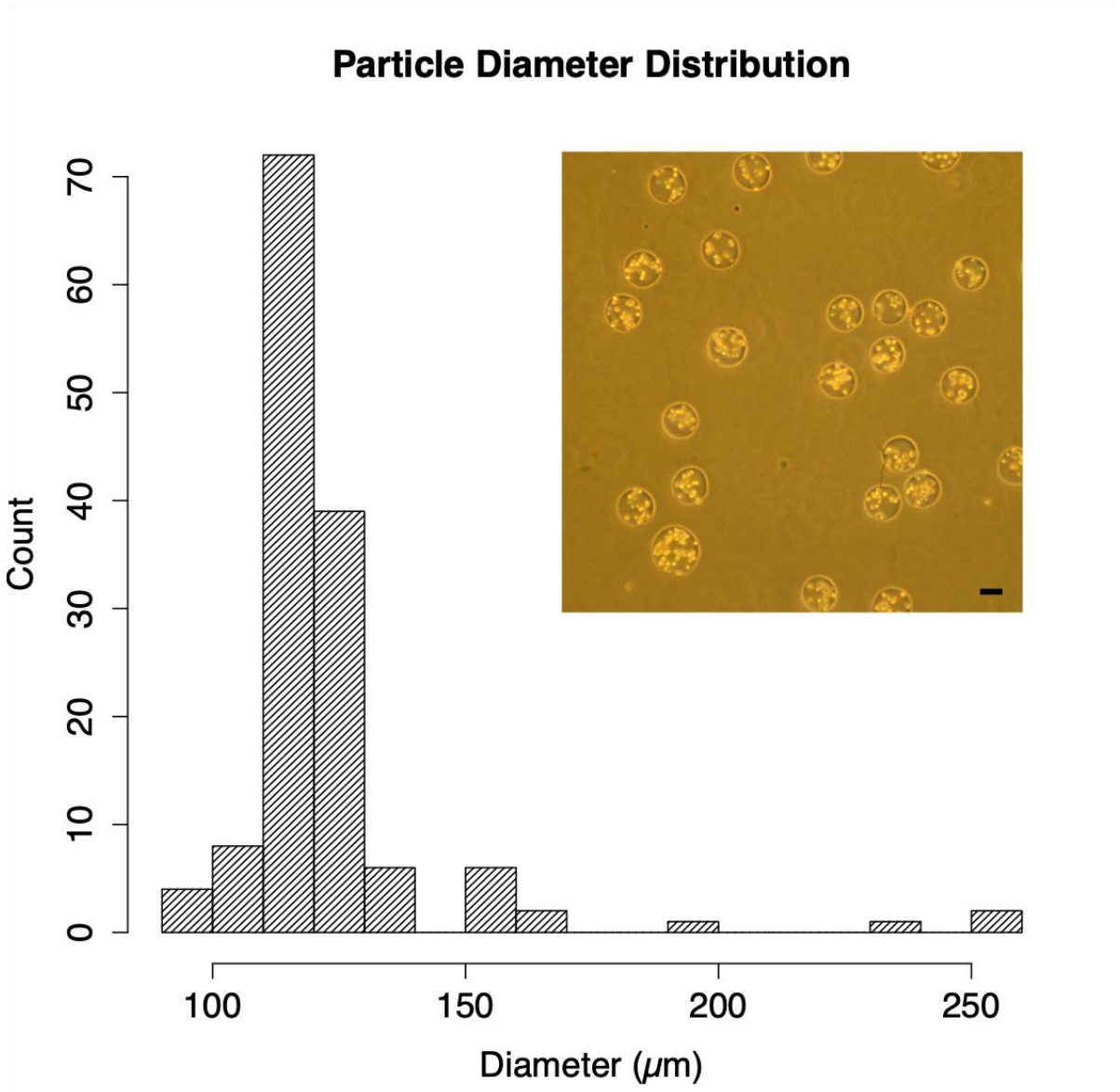

Figure S8. Particle size distribution of hydrogels encapsulating cells. The population of hydrogels is collected after crosslinking but before transferring to the suspension culture. A small volume of the hydrogel-containing solution is pipetted onto a glass slide, the hydrogels are imaged using brightfield microscopy, and measured using ImageJ. The population measured consisted of n = 140, average diameter of 124 µm, CV of 18.3%. Inset is a representative image of cell encapsulating hydrogels collected and imaged immediately after solidification in the calcium ion bath, demonstrating the size dispersity of the population as well as cell occupancy (scale bar = 50 µm).